

## FEM Analysis, Design and Optimization of a Compact Bandpass Filter for Low-power UWB Communications Applications

NADIA BENABDALLAH<sup>1</sup>, NASREDDINE BENAHMED<sup>2</sup> and FETHI TARIK BENDIMERAD<sup>2</sup>

<sup>1</sup> Department of Physics, Preparatory School of Sciences and Technology (EPST-Tlemcen), Tlemcen, Algeria

<sup>2</sup> Department of Telecommunications, University of Tlemcen, P. O. Box 119, (13000) Tlemcen, Algeria

### ABSTRACT

With the aid of the finite element method (FEM) and a commercial EM simulator, the analysis, the design and the optimization of a compact bandpass filter using interdigital coupled microstrip lines with performance suitable for low-power UWB communications applications, are presented.

The design of the compact UWB bandpass filter is based on the use of impedance steps and coupled-line sections, whereas the simulation of its frequency response ( $[S]$ ) is done using MATPAR software and it is based on the electromagnetic (EM) parameters for each section of line forming the bandpass structure.

The center frequency around 6.85 GHz was selected, the bandwidth is between 2.5-10.2 GHz, the insertion-loss amounts to 0.15 dB and the return loss is found better than 15 dB over a large portion of bandwidth.

For the selected center frequency and on RT/Duroid 6006 substrate with a dielectric constant of 6.36, our UWB BPF is only  $2.0 \times 1.524 \times 36.6$  mm in size.

### KEYWORD

Analysis design and simulation, compact filter; EM-parameters; FEM calculations; interdigital coupled microstrip lines; MATPAR software; UWB bandpass filter; S-parameters.

### 1. INTRODUCTION

ULTRAWIDEBAND (UWB) communications offers great promise for voice, video, and high-data-rate transmissions, although key components will be needed for such systems. One of those components is the bandpass filter (BPF).

Since the release of the frequency band from 3.1 to 10.6 GHz for commercial purposes by the US Federal Communications Commission (FCC) [1], UWB technology has sparked a great deal of interest for its potential in that band. Compact bandpass filters are essential components for UWB systems and have been studied through the use of the matured filter theory [2] and other techniques [3-4]. On the basis of impedance steps and coupled-line sections as inverter circuits, several works were interested in the design of planar broadband filters with low loss, compact size, high suppression of spurious responses, and improved stopband performances [5-6].

In this work, we are interesting in the analysis, the design and the optimization of a compact ultra wideband (UWB) bandpass filter using interdigital coupled microstrip lines, convenient for low-power applications. In order to facilitate the study of such bandpass structure, we divided it to simple sections of lines which can be easily analyzed under FreeFEM environment [7] or using other EM software [8-10]. The design of the UWB filter is based on the use of impedance steps and coupled-line sections. The center frequency around 6.85 GHz was selected, the bandwidth is between 2.4-10.2 GHz, the insertion-loss amounts to 0.15 dB and the return loss is found better than 15 dB in a large frequency range (3.0-9.5) GHz. For the selected center frequency and on RT/Duroid 6006 substrate with a dielectric constant of 6.36, our UWB BPF is only  $2.0 \times 1.524 \times 36.6$  mm in size. What follows are the analysis, the design and the optimization of this compact UWB filter using both FEM method under FreeFEM environment and MATPAR software [11].

### 2. UWB BANDPASS FILTER STRUCTURE

Figure 1-a shows the layout of a wideband bandpass filter using conventional interdigital coupled microstrip lines with RT/Duroid 6006 substrate, which has a dielectric constant of 6.36 and a thickness of 1.524mm. In order to facilitate the analysis and the design of such structure, we divided it to five sections of lines (Figure 1-b). The cross-sections of the lines forming the BPF with their geometrical dimensions in millimeters are shown in figure 2 and are assumed to propagate a quasi transverse electromagnetic mode (quasi-TEM) with low losses.

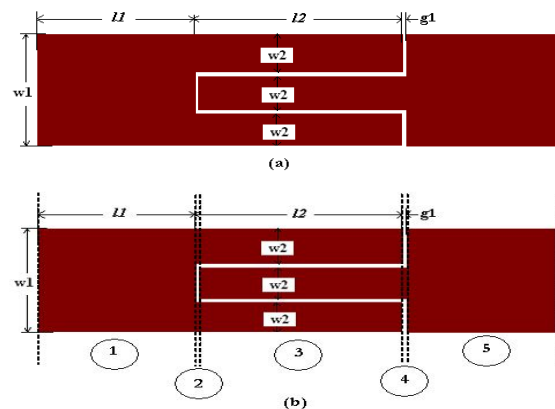
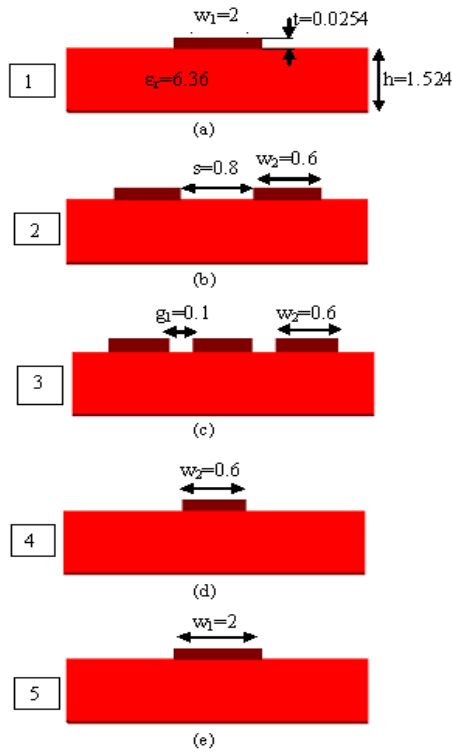
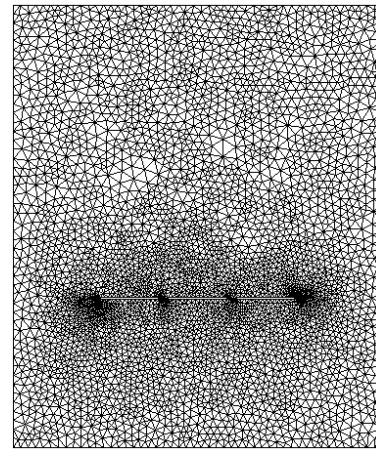


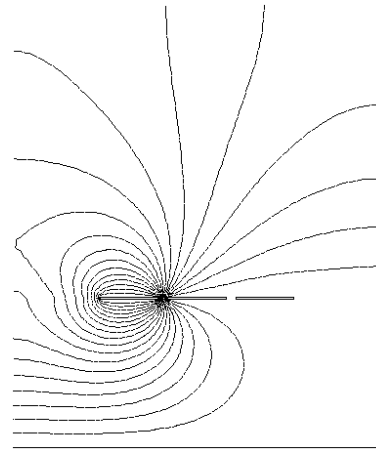
**Figure 1.** Bandpass structure: layout on (a) and sections representation on (b).



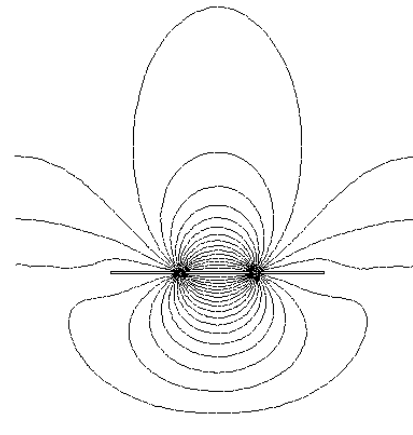
This solution represents the distribution of the potential  $V$  at the different mesh nodes of the quasi-TEM multiconductor transmission line (Figures 3-c and 3-b).



(a)



(b)



(c)

**Figure 3.** FEM meshes of the third section of the BPF on (a) and potential distributions for two different boundary conditions on (b) and on (c).

**Figure 2.** Cross-sections of each line forming the bandpass structure (dimensions are in mm).

### 3. ELECTROMAGNETIC PARAMETERS

The electromagnetic (EM) parameters of a multiconductor transmission line can be described in terms of its primary parameters [L] and [C].

Where:

$$[L] = \begin{bmatrix} L_{11} & \dots & L_{1n} \\ \vdots & & \vdots \\ L_{n1} & \dots & L_{nn} \end{bmatrix} \quad [C] = \begin{bmatrix} C_{11} & \dots & C_{1n} \\ \vdots & & \vdots \\ C_{n1} & \dots & C_{nn} \end{bmatrix}$$

The inductance matrix [L] contains the self-inductances of the n-conductor on the diagonal, and the mutual inductances between conductors in the off-diagonal terms.

Matrix [C] accounts for the capacitive effects between the n-conductor, characterizing the electric field energy storage in the quasi-TEM multiconductor transmission line.

For the studied structure, the coefficients of these matrices are obtained by solving a two-dimensional static field problem using FEM [12-13]. For each section of line, the solution is obtained by solving the Laplace's equation (Figure 3-a):

$$\text{div} [\nabla_t V(x, y)] = 0 \tag{1}$$

Subject to:

$V = 1$  Volt on the  $i^{\text{th}}$  conductor's surface.

$V = 0$  on all others conductors.

When the potential  $V$  is known, we calculate the  $i^{th}$  row of the  $[C]$  matrix from the electric charge on each conductor.

$$C_{ij} = (1/V_0) \int_{l_j} q_s dl \quad (2)$$

Where  $V_0 = 1\text{Volt}$ ,  $q_s = \epsilon_0 \epsilon_r E_N$ ; ( $\epsilon_r = 1$ ),  $l_j$  represents the contour around the  $j^{th}$  conductor and  $E_N$  is the normal component of the electric field.

In the high-frequency limit, i.e. the skin depth is sufficiently small such that current flow occurs only on the surface of the conductors, the inductance matrix  $[L]$  can be obtained from the matrix  $[C_0]$  [14]. The inductance matrix in terms of  $[C_0]$  calculated for ( $\epsilon_r = 1$ ) is:

$$[L] = \mu_0 \epsilon_0 [C_0]^{-1} \quad (3)$$

When the EM-parameters are determined, it is possible to estimate the scattering parameters ( $S_{11}$  and  $S_{21}$ ) of the analyzed UWB BPF shown in Fig. 1 using MATPAR software. This computer program was realized for the analysis of networks consisting of a number of multiconductor transmission lines and discrete linear elements. Each lossless transmission line is described by its matrix parameters ( $[L]$  and  $[C]$ ) and length, which are assumed to be known. The whole network has one or more ports, and it is analyzed in the frequency domain, at a set of discrete frequencies. The results of the analysis are the scattering parameters  $[S]$  of the network. The output of the program is similar to the results obtained in measurements on multiport networks using network analyzers [11].

#### 4. EM ANALYSES AND DESIGN

As part of this study on UWB microstrip lines bandpass filters, we examined the design of a  $50 \Omega$ -UWB filter having:  $w_1=2\text{mm}$ ,  $w_2=0.6\text{mm}$ ,  $g_1=0.1\text{mm}$ ,  $s=0.8\text{mm}$  and  $l_1=l_2=6.4\text{mm}$ . Using our computer programs done under FreeFEM environment for each section of line forming the studied UWB BPF, we obtained the EM-parameters listed into table1.

**Table 1.** EM Parameters of Each Section of Line of the UWB BPF

| Section of line | $[L]$<br>(nH/m)   | $[C]$<br>(pF/m)   |
|-----------------|---|---|
| 1               | 369,5   | 135.4   |
| 2               | $\begin{bmatrix} 586.6 & 185.0 \\ 185.0 & 586.6 \end{bmatrix}$  | $\begin{bmatrix} 82.25 & -18.5 \\ -18.5 & 82.25 \end{bmatrix}$  |
| 3               | $\begin{bmatrix} 549.1 & 321.9 & 219.6 \\ 321.9 & 528.1 & 321.9 \\ 219.6 & 321.9 & 549.1 \end{bmatrix}$ | $\begin{bmatrix} 113.3 & -56.76 & -5.1 \\ -56.76 & 145.8 & -56.76 \\ -5.1 & -56.76 & 113.3 \end{bmatrix}$ |
| 4               | 591.1   | 77.6  |
| 5               | 369.5   | 135.4   |

Under MATPAR environment, the equivalent representation of our UWB BPF is shown into the interconnecting network given in figure 4.

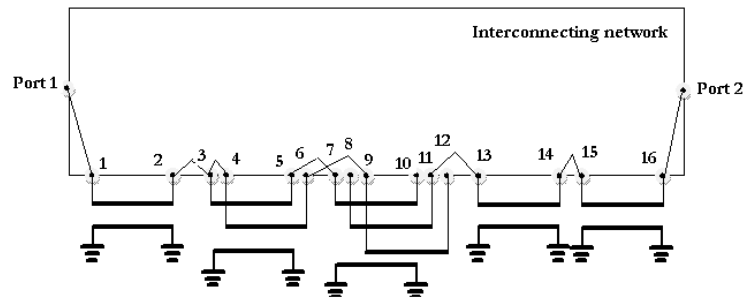


**Figure 4.** Equivalent representation of the UWB BPF under MATPAR environment.

After the introduction of the EM matrices and length of each section of line forming the UWB BPF, the interconnecting definition screen of MATPAR for the network of figure 4, looks as shown below.

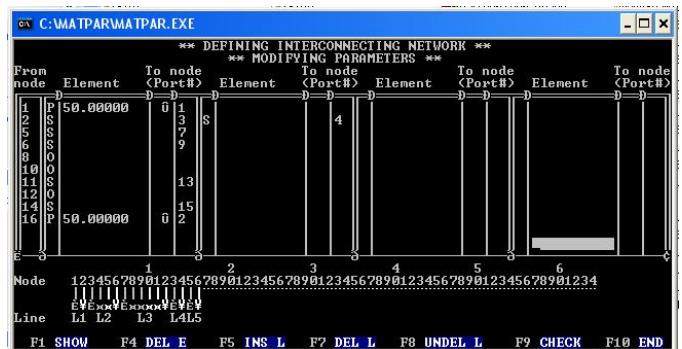


**Figure 5.** Interconnecting definition screen for the network of figure 4.

MATPAR software was applied to check the predicted electrical performance of our designed filter characterized by the geometrical parameters cited above. Figure 6 provides plots of the simulated scattering parameters ( $S$ -parameters) for the BPF from 1.0 to 12.5 GHz. The simulated results indicate passband insertion loss of about 0.47 dB with return loss of better than 10 dB from 4.0 to 9.0 GHz.

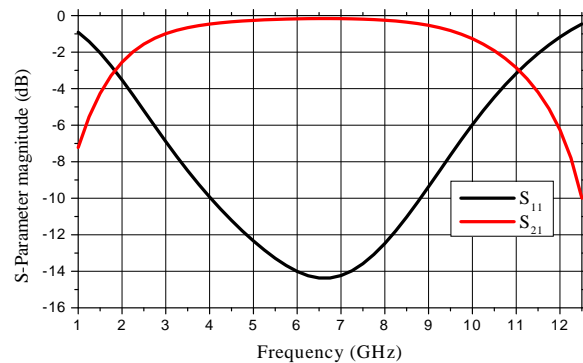


**Figure 6.** Scattering parameters of the designed  $50 \Omega$ -UWB BPF obtained by MATPAR software.

**5. OPTIMIZATION AND RESULTS**

The optimized interdigital coupled lines must be performed to achieve design-specified coupling factor between two adjacent line resonators. The usual procedure is to reduce strip width (from 0.6 to 0.2 mm) in order to achieve a tight coupling and lower insertion. Figure 7 gives our results obtained by FEM and MATPAR for strip width ( $w_2$ ) varying from 0.6 to 0.2 mm.

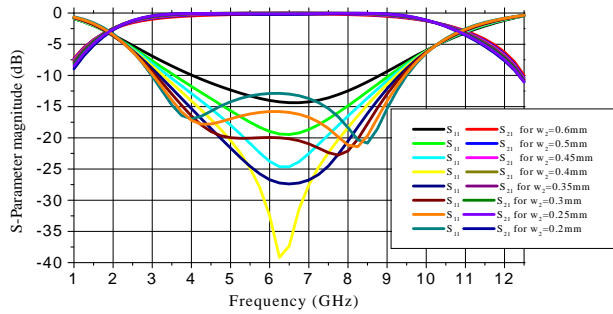


**Figure 7.** Scattering parameters of the designed 50 Ω-UWB BPF for different values of strip width ( $w_2$ ).

It can be noticed that all the interdigital coupled lines have almost the same resonant frequency and the same  $S_{21}$ . Nevertheless, the coupled line with  $w_2=0.4$ mm has superior performances with better  $S_{11}$  in the passband. This means that the new interdigital coupled line of  $w_2=0.4$ mm with EM-parameters listed into table 2 is more suited for use as a bandpass filter element than the others.

**Table 2.** EM Parameters of the Two Sections of the Interdigital Coupled Line of the Optimized UWB BPF

| Section of coupled line | [L]<br>(nH/m)   | [C]<br>(pF/m)   |
|-------------------------|---|---|
| 2                       | $\begin{bmatrix} 660.2 & 242.9 \\ 242.9 & 660.2 \end{bmatrix}$  | $\begin{bmatrix} 74.0 & -21.1 \\ -21.1 & 74.0 \end{bmatrix}$  |
| 3                       | $\begin{bmatrix} 628.9 & 382.3 & 272.3 \\ 382.3 & 611.6 & 382.3 \\ 219.6 & 382.3 & 628.9 \end{bmatrix}$ | $\begin{bmatrix} 101.0 & -51.8 & -6.7 \\ -51.8 & 130.0 & -51.8 \\ -6.7 & -51.8 & 101.0 \end{bmatrix}$ |

We applied the MATPAR software in the aim of checking the electrical performance of Two-resonator bandpass filters using the new interdigital coupled line. Our two-resonator BPF is characterized by the features marked in figure 8.

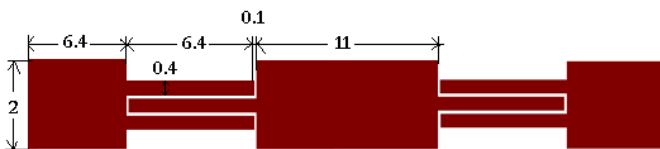


**Figure 8.** Longitudinal section view of the designed Two-resonator UWB BPF (Units in mm) .

Figure 9 illustrates a comparison of simulated responses ( $S_{11}$  and  $S_{21}$ ) of one- and two-resonator bandpass filters, in the frequency band [1.0-12.5] GHz. It can be seen that the optimized two-resonator bandpass filter has an insertion loss of about 0.15 dB with a return loss of better than 15 dB from 3.1 to 9.5 GHz. This last simulated response is in reasonable agreement with results of planar structures and it also meets the requirements for UWB applications per the FCC.

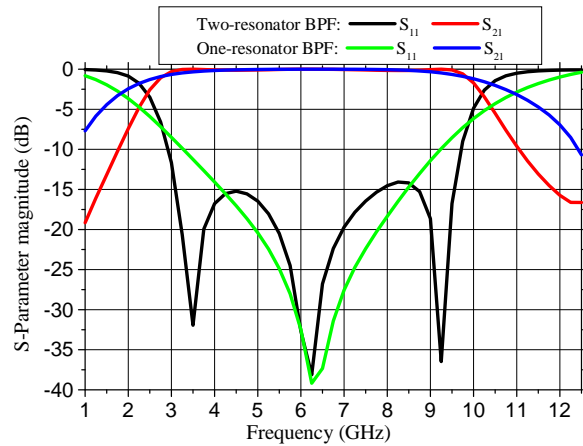


**Figure 9.** Scattering parameters of the designed and optimized 50 Ω-structures using one- and two-resonator bandpass filters.

**6. CONCLUSION**

In summary, this work presented the analysis, the design and the optimization of a compact ultra wideband bandpass filter using interdigital coupled microstrip lines, with performance suitable for low-power UWB communications applications.

The filter, which measures just  $2.0 \times 1.524 \times 36.6$  mm, was fabricated using RT/Duroid 6006 substrate by means of impedance steps and interdigital coupled-line sections.

It was designed with the aid of our programs done under FreeFEM environment and with the aid of MATPAR software, although other commercial EM simulation software can also be used.

The filter features a bandwidth between 2.5 to 10.2 GHz with better than 15 dB return loss and about 0.15 dB insertion loss over a large portion of bandwidth.

**REFERENCES**

1. FCC, Revision of Part 15 of the Commission's Rules Regarding Ultra-Wideband Transmission System, Technical Report ET-Docket 98-153, 14 February 2002.
2. G. Matthaei, L. Young, and E. M. T. Jones, Microwave Filters, Impedance-Matching Networks, and Coupling Structures, Norwood, MA: Artech House, 1980.

3. A. Saito, H. Harada, and A. Nishikata, "Development of bandpass filter for ultra wideband (UWB) communication," in Proc. IEEE Conf. Ultra Wideband Syst. Tech., 2003, pp.76-80.
4. L. Zhu, S. Sun, and W. Menzel, "Ultra-wideband (UWB) bandpass filters using multiple-mode resonator," IEEE Microw. Wireless Compon. Lett., Vol. 15, No. 11, Nov. 2005, pp. 796-798.
5. J. Gao, L. Zhu, W. Menzel and F. Bögelsack, "Short-Circuited CPW Multiple-Mode Resonator for Ultra-Wideband (UWB) Bandpass Filter," IEEE Microw. Wireless Compon. Lett., Vol. 16, No. 3, March 2006, pp. 104-106.
6. M. Meeloon, S. Chaimool and P. Akkaraekthalin, Broadband bandpass filters using slotted resonators fed by interdigital coupled lines for improved upper stopband performances, Int J Electron Commun (AEU) (2008).
7. www.Freefem.org
8. A. Benkaddour, N. Benahmed, N. Benabdallah and F.T. Bendimerad, "Create UWB Filters With Coaxial Cables," Microwaves & RF, Vol. 51, No 7, July 2012, pp. 59-63.
9. N. Benahmed, N. Benabdallah, S. Seghier, F.T. Bendimerad and B. Benyoucef, "Analyzing an UWB Bandpass Filter for High Power Applications Using Rectangular Coaxial Cables with Square Inner Conductors," Circuits and Systems (CS), Vol. 2, No. 3, pp. 121-126, July 2011.
10. A.R. Djordjevic, M.B. Bazdar, T.K. Sarkar, LINPAR for windows: Matrix parameters of multiconductor transmission lines, Software and user's manual, Artech House, 1999.
11. A.R. Djordjevic, M. Bazdar, G. Vitosevic, T. Sarkar and R.F. Harrington, Scattering parameters of microwave networks with multiconductor transmission lines, Artech House, 1990.
12. N. Benabdallah, N. Benahmed, S. Seghier and R. Bouhmidi, "Sliced coaxial cables form compact couplers," Microwaves and RF, Vol. 46, No. 7, July 2007, pp.90-94.
13. N. Benahmed and S. Seghier, "Rigorous analytical expressions for the electromagnetic parameters of rectangular coaxial couplers with circular and square inner conductors," Microwave Journal, Vol. 49, No. 8, August 2006, pp. 164-174.
14. K. Aliane, N. Benabdallah, N. Benahmed, R. Bouhmidi and F.T. Bendimerad, "Analysis and Design of a Quasi-TEM Slotted Tube Resonator for UHF-MRI," International Journal of Modern Engineering Research (IJMER), Vol.2, Issue.2, Mar-Apr 2012, pp-233-238.